

BRIEF REPORT



Tumor-infiltrating lymphocytes-derived CD8⁺ clonotypes infiltrate the tumor tissue and mediate tumor regression in glioblastoma

Lucas C. M. Arruda pa,b*, Julia Karbachc*, Dragan Kiselickic, Hans-Michael Altmannsbergerd, Evgueni Sinelnikov^e, Dirk Gustavus^e, Hans Hoffmeister^e, Akin Atmaca^c, and Elke Jäger^c

^aDepartment of Medicine Huddinge, Karolinska Institutet, Stockholm, Sweden; ^bCuraCell, Solna, Sweden; ^cDepartment of Oncology and Hematology, Krankenhaus Nordwest, Frankfurt am Main, Germany; Institute of Pathology, Krankenhaus Nordwest, Frankfurt am Main, Germany; eZellwerk GmbH, Eichstaedt, Germany

ABSTRACT

Adoptive cell therapy with tumor-infiltrating lymphocytes (TILs) has demonstrated consistent clinical efficacy in treating advanced melanoma and other "hot" tumors. However, it has shown limited success in "cold" tumors like glioblastoma. We present the successful treatment of a rapidly progressing glioblastoma patient with TILs expanded using a defined cytokine combination of IL-2, IL-15, and IL-21. The patient received lymphodepletion with cyclophosphamide one day pre-TIL infusion, followed by a single dose of IL-2 post-transfer. Complete tumor regression was observed after two TIL infusions administered two weeks apart. The TIL products were enriched for CD8⁺ T-cells and demonstrated specific lysis of the autologous tumor cell line. Transcriptomic analysis of tumor biopsies post-TIL infusion revealed increased expression of genes associated with immunological synapse formation and T-cell effector function, correlating with the patient's clinical outcome. T-cell receptor (TCR) next-generation sequencing of the infused TILs and post-treatment tumor biopsies confirmed the infiltration and expansion of TIL-derived clonotypes within the tumor microenvironment. CD8⁺ T-cell clonotypes exhibited robust tumor migration and expansion, while CD4⁺ T-cells showed limited tumor infiltration. In conclusion, TILs expanded with IL-2/IL-15/IL-21 represent a promising therapeutic approach for glioblastoma, overcoming traditional challenges posed by the tumor microenvironment and achieving significant clinical outcomes.

SIGNIFICANCE

IL-2/IL-15/IL-21-expanded TILs achieved complete tumor regression in a high-TMB glioblastoma patient, overcoming the immunosuppressive microenvironment. This case highlights a novel approach for treating gliomas using tailored adoptive cell therapy strategies.

ARTICLE HISTORY

Received 10 June 2025 Revised 11 August 2025 Accepted 7 September 2025

KEYWORDS

Glioblastoma: tumorinfiltrating lymphocytes; IL-2; IL-15; IL-21; cytotoxic T- cells

Introduction

Adoptive cell therapy with tumor-infiltrating T lymphocytes (TIL) has achieved notable clinical success in melanoma, where durable responses have been observed even in advanced disease settings. Beyond melanoma, TIL therapy has also shown clinical benefit in patients with chemotherapy-refractory, immunologically "hot" tumors such as non-small cell lung and colorectal cancers. 2,3 Most recently, a randomized phase III trial established the superiority of TIL therapy over immune checkpoint blockade in advanced melanoma reinforcing its therapeutic potential. However, the extension of TIL therapy to immunologically "cold" tumors remains limited and warrants further investigation.

IDH-wildtype glioblastoma (GBM) is the most aggressive primary brain tumor in adults, characterized by a median survival of less than 15 months and a 5-year survival rate below 5%.⁵ Standardof-care therapy, comprising maximal safe resection surgery, radiotherapy, and temozolomide chemotherapy,⁶ offers only modest clinical benefit, and prognosis remains poor.⁵ Tumor recurrence

CONTACT Elke Jäger 🔯 ej200161@aol.com 🖻 Department of Oncology and Hematology, Krankenhaus Nordwest, Steinbacher Hohl 2-26, Frankfurt am Main 60488, Germany

*These authors contributed equally and share first authorship.

Supplemental data for this article can be accessed online at https://doi.org/10.1080/2162402X.2025.2559784

occurs in the vast majority of patients and complete remissions at this stage are rare exceptions. In this context, numerous immunotherapeutic strategies have been investigated, including immune checkpoint inhibitors, cancer vaccines, and adoptive cell therapies. However, clinical outcomes have been unsatisfactory. Adjuvant anti-PD-1 therapy administered alongside radiotherapy (plus temozolomide in methylated tumors) following surgery failed to demonstrate a benefit over the standard care. Similarly, although individualized vaccines can elicit tumor-specific T-cell responses in GBM, their clinical efficacy remains limited largely due to the tumors' immunologically "cold" phenotype.

Chimeric antigen receptor (CAR) T-cells therapies have recently been tested in GBM, with early-phase trials targeting tumor-associated antigens such as IL-13 Rα2, EGFRvIII, or B7-H3.⁷ Although peripherally infused CAR T-cells can cross the blood – brain barrier (BBB) and infiltrate the tumor tissue, clinical responses have been limited.¹² Consequently, most T-cell – based therapies are now predominantly administered via local delivery.^{13–16} In patients with recurrent GBM, repeated local delivery of IL-13 Rα2-targeted CAR T-cells achieved a disease control rate of approximately 50%¹⁵ and similarly encouraging results were reported with intracerebroventricular administration of B7-H3-directed CAR T-cells in diffuse intrinsic pontine glioma.¹⁶ In contrast, EGFRvIII-specific CAR T-cells have shown limited efficacy likely due to heterogeneous antigen expression and antigen loss under therapeutic pressure.¹² To overcome these limitations, next-generation strategies are being developed, including bivalent CAR constructs targeting both EGFRvIII and IL-13 Rα2,¹³ as well as CAR T-cells engineered to secrete T-cell-engaging antibody molecules to broaden tumor recognition and enhance bystander killing.¹⁴ While these innovations may improve tumor recognition and reduce the risk of immune escape, they also introduce new safety concerns, such as off-target toxicity and complications associated with invasive delivery methods.

TILs recognize a broad range of tumor antigens, including both patient-specific neoantigens and shared self-antigens, possess strong tumor-homing capacity and cytotoxic function, key features that underlie their clinical efficacy in solid tumors. ¹⁷ Unlike CAR T-cells, which are limited by the need for a single defined antigen, TIL products contain diverse T-cell receptor (TCR) specificities capable of targeting multiple tumor-specific antigens. ^{3,17,18} Their derivation from the tumor microenvironment further enhances their ability to traffic back to the tumor site upon reinfusion, ¹⁷ addressing both the antigenic heterogeneity and infiltration barriers that often limit CAR T-cell efficacy in GBM. In a pilot study, intrathecal administration of autologous TILs in combination with IL-2 was found to be safe and induced clinical responses in five of six patients with recurrent GBM. ¹⁹

In this case report, we describe the treatment of a patient with recurrent GBM using TILs expanded with IL-2/IL-15/IL-21 under a compassionate use protocol. We present immunogenomic data demonstrating TIL infiltration, clonal expansion, and tumor control following therapy. These findings highlight the potential of TIL therapy as a personalized treatment approach in GBM and support further clinical investigation of TIL-based immunotherapy in other central nervous system malignancies.

Material and methods

Isolation, cultivation and functional characterization of TIL

TILs were isolated from the GBM specimen and cultivated in CellGro medium (CellGenix Inc.) containing GMP-grade IL-2 (1000 IU/mL), IL-15 (180 IU/mL) and IL-21 (1 IU/mL) (Miltenyi Biotec GmbH, Germany), 10% GMP-grade human AB serum, supplemented with anti-CD3 (clone OKT3, 30 ng/mL, Miltenyi Biotec GmbH, Germany) and gamma-irradiated allogeneic feeder cells. Expansion and activation of TIL were performed in a closed perfusion bioreactor system. Flow cytometry was performed to evaluate the phenotype, degranulation (CD107a) and Treg enumeration prior to TIL infusion. IFN-γ production was tested by stimulating TIL with anti-CD3 for 24 hours followed by cytokine quantification in the culture supernatant by enzyme-linked immunosorbent assay (ELISA) and expressed as pg/1.0 x 10⁵ T-cells/24 hours. Specific lysis of the autologous GBM tumor cell line by TIL was measured in standard 4-hour Chromium-51 release assay. K562 leukemia cells, Daudi lymphoblast cell line and autologous EBV-transformed B-cells were used as controls. A full description of the TIL functional assays is provided below.



T-cell phenotype

Peripheral blood mononuclear cells or TIL were stained with the following antibodies: anti-human CD3 PE-Cy7 (BD Biosciences, Catalog Number: 563423), anti-human CD4 V450 (BD Biosciences, Catalog Number: 56345), anti-human CD8\alpha APC-Cy7 (BD Biosciences, Catalog Number: 557834), anti-human CXCR3 BD Horizon™ R718 (BD Biosciences, Catalog Number: 567038), anti-human CCR4 PE (BD Biosciences, Catalog Number: 551120), anti-human CCR6 BD Horizon™ BB515 (BD Biosciences, Catalog Number: 564479), anti-human CCR7 PE (BD Biosciences, Catalog Number: 560765) and anti-human CD45RA FITC (BD Biosciences, Catalog Number: 561882). Acquisition of events was performed using a BD FACS Canto II flow cytometer (BD Biosciences, Stockholm, Sweden). CD4⁺ T helper profile based on CXCR3/CCR4/CCR6 surface expression was performed as follow: Th1 (CXCR3⁺CCR6⁻CCR4⁻), Th2 (CCR4⁺CXCR3⁻CCR6⁻), Th17 (CCR4⁺CCR6⁺CXCR3⁻) and nonconventional Th1* (CXCR3+CCR6+CCR4-).21 T-cell differentiation subtypes were defined by CCR7 and CD45RA expression as naïve (CCR7+CD45RA+, TN), central memory (CCR7+CD45RA-, T_{CM}), effector memory (CCR7⁻CD45RA⁻, T_{EM}) or fully differentiated effector cells (CCR7⁻CD45RA⁺,

CD107a induction

TILs were incubated in RPMI medium (Gibco, Catalog Number: 61870-010) supplemented with 10% fetal bovine serum (FBS, Gibco 10,500-056), penicillin and streptomycin (Gibco, Catalog Number: 15140122), and 100 ng/ml phorbol 12-myristate 13-acetate (PMA, Sigma-Adrich, Catalog Number: P8139) for 2 hours at 37°C with 5% CO₂. The anti-human CD107a PE antibody (BD Biosciences, Catalog Number: 555801) and 4 µL of BD GolgiStop solution (BD Biosciences, Catalog Number: 554724) were also added to the cells during the incubation period in order to capture surface-bound CD107a molecules while halting their internalization. The cells were then washed and stained with the anti-human CD3 PE-Cy7, anti-human CD4 V450 and anti-human CD8α APC-Cy7 antibodies used in the T-cell phenotype assay. The stained cells were washed once again and acquired on a BD FACS Canto II flow cytometer. Assays were performed in triplicates and control cells (IL-15, IL-2 - activated T-cells) were included to assure quality control.

Regulatory T cells

TILs were stained with the following antibodies: anti-human CD3 PE (BD Biosciences, Catalog Number: 555333), anti-human CD4 V450 (BD Biosciences, Catalog Number: 56345), anti-human CD8α APC-Cy7 (BD Biosciences, Catalog Number: 557834), anti-human CD25 PE-Cy7 (BD Biosciences, Catalog Number: 335824) and anti-human CD127 APC (Beckman Coulter, Catalog Number: B42026). After washing, cells were treated with the TrueNuclear Transcription factor buffer (BioLegend, Catalog Number: 424401), followed by staining with anti-human FoxP3 Alexa 488 (BD Biosciences, Catalog Number: 560047). The cells were incubated for up to an hour, washed and acquired on a BD FACS Canto II flow cytometer (BD Biosciences, Stockholm, Sweden). Assays were performed in triplicates and PBMCs from a healthy donor showing 2% of Treg, defined as CD3+CD4+CD25highCD127, were used as positive control cells for immunostaining.

Chromium-51 release assay

Specific cytotoxicity was determined in standard chromium-51 (Cr⁵¹) release assays as previously described. 22 Briefly, autologous or control tumor cell lines ('target cells,' T) were labeled with 100 µ CiNa₂⁵¹CrO₄ for 2 hours. 1000 target cells were then incubated in V-bottom microwell plates with TIL ('effector cells,' E) at different E:T ratios for 4 h at 37°C. Chromium-51 release was measured in the supernatant and specific cytotoxic activity was calculated by the standard method which measures lysis of Cr⁵¹-labeled target cells (autologous tumor cell line) by the effector cells (TIL) based on the amount of radioactivity released into the supernatant. Allogeneic GBM cell lines U-373 (ATCC no: HTB-17) and DBTRG05 (ATCC no: CRL-2020), Daudi B-lymphoma cell line (ATCC no: CRL-213) and the autologous

EBV-transformed B cell line served as controls. For the cold target inhibition assays, a titration of the cold to hot tumor cells was done in the presence of 90:1 TIL. Following this, the TIL were pre-incubated at different ratios to the target cells with unlabeled autologous tumor cells as competitors at a ratio of 90:1 (cold:hot target) to block nonspecific reactivity.

Whole exome sequencing (WES)

Fresh-frozen tumor tissue material was sent to CeGaT (Tübingen, Germany) for WES. Library was prepared using the Agilent kit SureSelectXT Human All Exon V6 and sequenced in a NovaSeq 6000 (Illumina, 2×100 bp). Demultiplexing of the sequencing reads was performed with Illumina bcl2fastq (version2.20). Adapters were trimmed with Skewer (version 0.2.2). Sequencing data analysis was performed using the Illumina DRAGEN platform (version 4.2.4).

Transcriptome analysis

Fresh-frozen tumor tissue material was sent to CeGaT (Tübingen, Germany) for RNA sequencing. Library was prepared using the SMARTer Stranded Total RNA Seq Kit v2- Pico Input (Takara) and sequenced in a NovaSeq 6000 (Illumina, 2×100 bp). Demultiplexing of the sequencing reads was performed with Illumina bcl2fastq (version 2.20) and adapters were trimmed with Skewer (version 0.2.2). Trimmed raw reads were aligned to grch38 using STAR (version 2.7.3). Differential expression analysis between groups was performed with DESeq2 (version 1.24.0) Representation (GO) analysis was performed on differentially expressed genes. The gene list containing genes with a $\log_2 FC > 1.5$ and was used as input for the R package clusterProfiler (version 4.3.1.900).

T-cell receptor (NGS) next-generation sequencing (NGS)

Sorted CD4 $^+$ and CD8 $^+$ T-cells from TIL products and peripheral blood samples, and fresh-frozen tumor tissue material were sent to iRepertoire (Huntsville, AL) for TCR NGS. In brief, RNA reverse transcription was conducted with a one-step reverse transcription and the PCR product was purified. A multiplex secondary amplification was performed allowing addition of Illumina adapter sequences. Libraries were purified and sequenced in an Illumina MiSeq following standard TCR NGS guidelines. Sequencing data in fastq format were uploaded to the iRepertoire webserver (https://irweb.irepertoire.com/ir/index) for V(D)J recombination alignment in the TCR β chains. Complete mapped sequencing data was analyzed using Immunarch (https://immunarch.com/index.html), including TCR diversity, overlap, spectratype and clonotype tracking.

Imaging

Diffusion-weighted magnetic resonance imaging (DWI-MRI) with apparent diffusion coefficient (ADC) or computed tomography (CT) with enhancement (following contrast agent administration) was used to gauge the radiological follow-up prior and post-TIL therapy.

Histology

Formalin-fixed paraffin-embedded tumor samples were collected before and after TIL treatment. Tissue sections were deparaffinized and rehydrated, and IHC was performed using the Leica BOND Protocol (Leica Biosystems, Nussloch, GmbH) following the manufacturer's instructions. In brief, antigen retrieval was performed using BOND epitope retrieval ER2 solution for 20 minutes at 100°C followed by peroxide and protein block. Staining for p53 was performed using the *in vitro* diagnostic kit for p53 detection (catalog number: P53-DO7-L-U), comprising the mouse antihuman protein p53 (clone DO-7), diluted 1:800 for 30 minutes at 25°C, and visualized using the BOND Polymer Refine detection kit (Leica Biosystems) with diaminobenzidine (brown color).

Rabbit anti-human C-terminal CD8 antibody (clone EP1150Y), diluted 1:500 for 30 minutes at 25°C, was used to assess T-cell infiltration in the tumor samples. Visualization was performed using BOND Polymer Refine Red detection kit (Leica Biosystems) with Fast Red chromogen (red color) to allow the dual staining of p53 and CD8. Slides were counterstained with hematoxylin for nuclei visualization.

Ethics approval and patient consent

Ethics approval was not required, as single-patient compassionate use in Germany is not subject to ethics committee oversight. Study participant provided informed consent before taking part, including consent for publication.

Results

Case presentation

A 75-year-old male with pretreated non-methylated glioblastoma, IDH wild type, WHO grade 4, presented with recurrent disease after 12 months of initial diagnosis. Initial treatment included surgical resection, radiotherapy (34 Gy) with concurrent temozolomide in accordance with the standard Stupp protocol, 6 and subsequent adjuvant temozolomide for six cycles. One-month later, the patient presented with recurrent disease and was treated with lomustine for one month without clinical benefit. The patient requested the evaluation of TIL therapy and was admitted to the hospital. As a debulking approach and to isolate TILs, the recurrent tumor was subtotally resected. At the time of surgery, the patient's clinical status was consistent with a Karnofsky Performance Status (KPS) of 80, with preserved cognitive function, intact speech, and moderate hemiparesis. Postoperative recovery was uneventful without relevant neurological senso-motoric deficiencies. The patient remained neurologically stable, with no new focal deficits and maintained full consciousness throughout the immediate postoperative period. In the absence of effective alternative treatment options and to limit tumor progression during the TIL manufacturing period, temozolomide therapy was reinitiated as a bridging strategy following surgery. This was intended to provide disease control while the TIL product was being prepared for infusion.

Six weeks later, the patient presented with impaired neurological symptoms, e.g., mild motoric aphasia, ataxic gait and partial defect of visual field. In the cranial MRI, a recurrent and significantly progressive disease was observed with a part of the tumor growing into the brain stem and TIL treatment was initiated.

To promote engraftment of the transferred TIL product, the patient received reduced-dose cyclophosphamide (60 mg/kg, i.v.) one day prior to each TIL infusion, aiming to deplete regulatory T-cells and create a favorable immunologic niche. 31 The next day, 0.7x109 TIL (TIL-1) were administered by the intravenous route (i.v.) within 45 min. The TIL infusion was supported with a single dose of IL-2 (60,000 IU/kg, i.v.) administered 8 hours later to enhance survival and functional persistence of the transferred T-cells. 32 Given the occurrence of compartmentalized inflammation within the intracranial space, the patient subsequently received tocilizumab (anti - IL-6 receptor, 4 mg/kg, i.v.) and etanercept (soluble TNF receptor, 25 mg, subcutaneously. These were administered 24 hours after the first TIL infusion and 72 hours after the second infusion, following strategies adapted from CAR-T and adoptive cell therapy protocols where cytokine release syndrome (CRS) may occur³³ (Figure 1A). All medications were administered under compassionate use authorization and were provided at no cost to the patient. This preconditioning and supportive regimen was selected to balance immune activation with safety in the context of heavily pretreated glioblastoma. The patient was closely monitored for adverse events (AEs) and clinical development by MRI or CT according to immunotherapy Response Assessment in Neuro-Oncology (iRANO) recommendations.³⁴

On day + 1 post-infusion, the patient's clinical status deteriorated to a KPS of approximately 40, with somnolence, reduced consciousness, confusion, and worsening hemiparesis. In parallel, imaging revealed an increase in tumor mass and surrounding edema, suggesting elevated intracranial pressure. Urgent surgical decompression and partial tumor resection was performed to avoid fatal increase of intracranial pressure. Postoperatively, the patient's consciousness improved, with a partial clinical recovery to KPS 60, although cognitive impairment, aphasia, and motor deficits persisted.

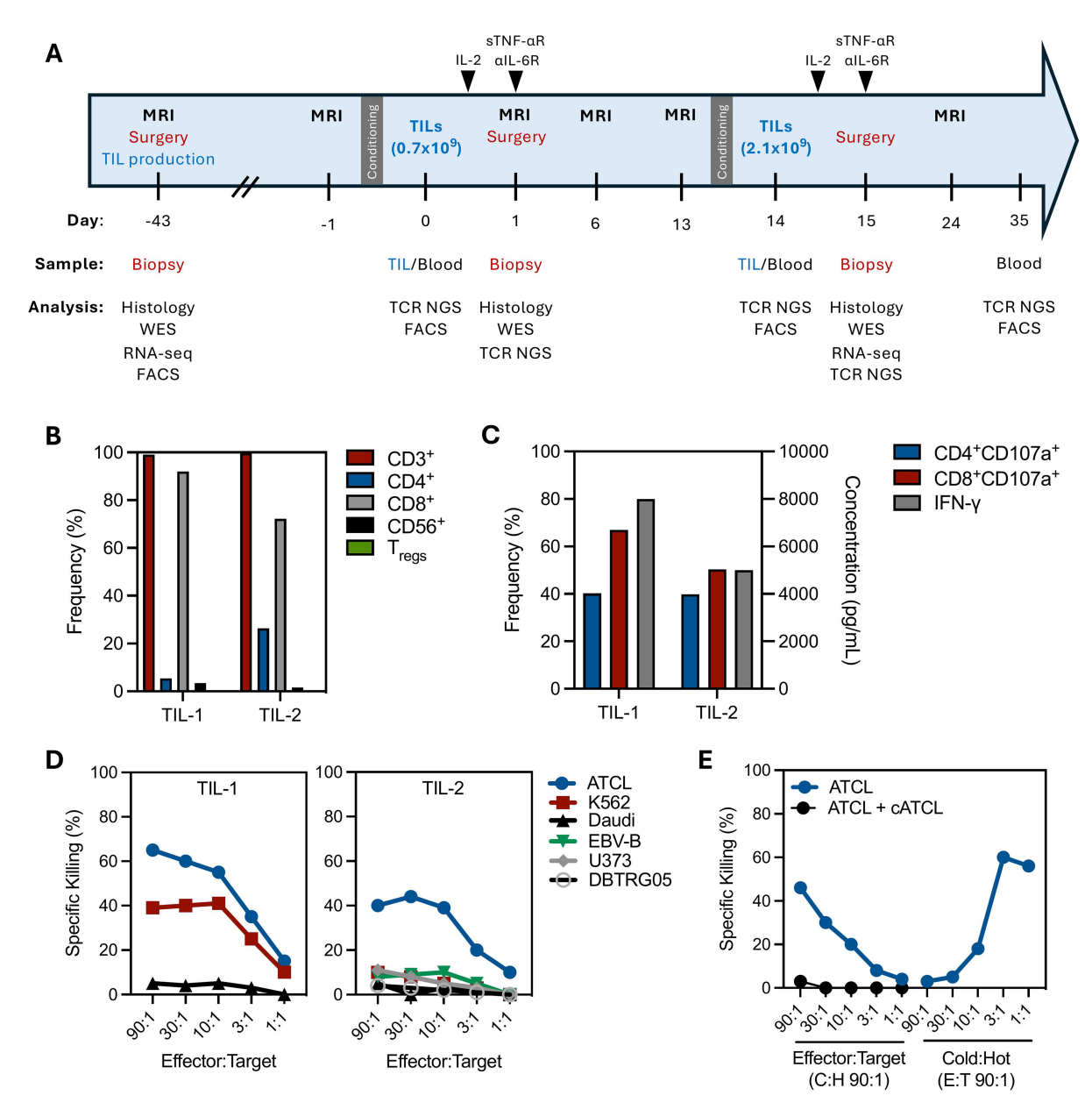


Figure 1. Treatment schedule and TIL product characteristics. (A) Treatment schedule indicating TIL infusion and cyclophosphamide administration. A partial resection of the GBM tumor in the patient's occipital lobe was performed 6 weeks prior to TIL-1 infusion (day -43) to obtain tissue for TIL manufacturing. The patient was treated with 60 mg/kg cyclophosphamide (CTX) one day prior to TIL infusion on either occasion (TIL-1 and TIL-2 infusions). Eight hours after TIL infusion, IL-2 (60,000 IU/kg) was administered i.V., followed by anti-TNF-α (soluble TNF receptor, etanercept, 25 mg) s.C. And anti-IL-6 receptor (IL-6 R, tocilizumab, 4 mg/kg) i.V. To prevent systemic hyperinflammatory reactions 24 and 72 hours after TIL-1 and TIL-2 infusion, respectively. Serial sampling was performed to assess tumor mutation burden, transcriptomics and TIL persistence/ infiltration analysis. (B) Flow cytometric analysis of T-cell phenotypes (CD4⁺ and CD8⁺) and contaminants evaluation (CD56⁺ NK-cells and tregs) in manufactured TIL products. (C) CD107a induction in CD4⁺/CD8⁺ T-cells post-PMA stimulation and IFNγ production in TIL products after 24-hours stimulation with OKT3 were used to gauge TIL functionality prior to infusion. (D) Cytotoxic potential of the TIL products as assessed by standard chromium release. Cr51-labeled autologous tumor cell line (ATCL) or control tumor cell lines (targets) were incubated with tumor-infiltrating lymphocytes (TILs, effectors) at varying effector-to-target (E:T) ratios, and cytotoxic activity was calculated based on Cr⁵¹ release into the supernatant. Controls included allogeneic GBM cell lines (U-373, DBTRG05), Daudi B-lymphoma cell line and autologous EBV-transformed B-cell line. (E) Cold target inhibition assays using a constant E:T ratio of 90:1, varying cell numbers of cold tumor cells were incubated with hot tumor cells to titrate the blocking of TIL activity. Highest blocking was commensurate in the presence of higher numbers of cold tumor cells (up to almost 100% at 90:1 and approximately 95% at 30:1) co-incubated with hot tumor cells. A set ratio of cold:hot tumor cell was used (90:1) to gauge TIL activity at varying cell numbers of TILs.

Despite initial clinical deterioration early post-TIL-1, follow-up MRI revealed a significant reduction in solid tumor volume with signs of central necrosis, suggesting a partial therapeutic response yet with the tumor still invading into the brain stem. After clinical stabilization (KPS 60) and in agreement with the patient and family, a second TIL infusion (TIL-2) was administered on day + 14 to enhance therapeutic efficacy and capitalize on the observed radiologic changes. The decision to proceed was based on the absence of progressive neurological decline, imaging evidence of treatment effect, and tolerance to the first TIL infusion.

The second TIL treatment was administered on day 14 with 2.1x10⁹ TILs (TIL-2) with cyclophosphamide treatment on day -1 and IL-2 administration 8 h post TIL. Tocilizumab plus etanercept were administered to prevent further hyper-inflammatory reactions 72 hours post-second TIL infusion. On day 2 post TIL-2, the cranial imaging showed an increase of intracranial pressure mainly caused by necrotic transformation of the tumor mass. Necrosectomy was performed the same day and subjected to histopathological analysis. Sequential cranial MRI showed complete tumor remission. Further treatment of the patient focused on rehabilitative and supportive care. The patient died 2 months after the first TIL therapy and 15 months after initial diagnosis from non-disease-related causes.

Clinical outcome

Serial imaging revealed rapid tumor progression prior to TIL therapy, followed by extensive tumor necrosis and radiologic regression after treatment. The patient's first MRI at 6 weeks before first TIL infusion (T2, before partial resection) showed a tumor with a cystic temporal component surrounded by a solid mass extending into the left parietal region. The mass showed initial signs of a midline shift to the right without herniation. Diffusion-weighted imaging (DWI) and apparent diffusion coefficient (ADC) sequences showed diffusion restriction, with dense packing of cells representing a high degree of malignancy.

The next MRI at day -1 pre-TIL-1 infusion showed a massive progression of the solid lesion in all sequences (T2, DWI, ADC, Flair, T1 after contrast agent administration). The midline shift to the right revealed temporal herniation risk, with massive diffusion restriction of the solid lesion (DWI and ADC) with the tumor reaching into the mesencephalon.

At day + 1 after TIL-1 infusion, a CT scan was performed instead of an MRI due to the patient's critical condition. In the contrast-enhanced CT scan of the brain, a central necrotic lesion juxtaposed to the hemicraniectomy within the left parietal portion was visible, with reduced enhancement in the solid tumor. This was consistent with early intratumoral necrosis.

Subsequent MRIs demonstrated progressive radiologic changes suggestive of treatment response. The MRI on day + 2 showed T2 shine through in the ADC sequence, representing vasogenic edema instead of diffusion restriction. This was confirmed by DWI and ADC on day + 6 after TIL-1 infusion. The MRI on day + 13 (post-TIL-1) showed a shrunken solid tumor dominated by a central necrotic portion (T2 sequence), depicted by the high signal intensity in ADC representing T2 shine through and highlighting loss of cellular density. An MRI performed 10 days post-TIL-2 infusion showed a dead cell mass in the solid tumor (T2 image). Biopsies of the tumor show complete necrotic tissue transformation.

Due to brain compression symptoms after TIL-1 and TIL-2 transfer, surgical decompression was performed repeatedly. The multiple neurosurgical interventions were not preplanned components of the TIL protocol, but were conducted as urgent clinical measures in response to tumor-associated mass effect, edema, and signs of increased intracranial pressure. Each procedure was performed only after comprehensive discussion with the patient and his family, who provided explicit informed consent based on evolving clinical findings.

Safety

The patient tolerated the two TIL infusions and associated treatments without life-threatening toxicities. Cardio-respiratory parameters and core temperature remained stable throughout treatment (Supplementary Figures S1-S2), and no signs of cytokine release syndrome (CRS), hypotension, or respiratory compromise were observed. Hematological analyses revealed persistently low lymphocyte and monocyte counts (< 2 cells/μL) despite the use of reduced conditioning regimen, while leukocyte and neutrophil counts peaked during TIL transfers and dropped post-IL-2, recovering with filgrastim (G-CSF; Supplementary Figure S3). No febrile neutropenia or infectious complications were recorded. Liver function markers showed transient elevations, with GGT peaking at ~250 U/L and AST at ~120 U/L, both normalizing two weeks after TIL-2 infusion (Supplementary Figure S4). These findings were consistent with reversible cytokine-mediated hepatotoxicity. Renal function remained within normal range throughout. A surge in serum IL-6 and sIL-2 R levels was seen immediately after each TIL infusion, indicating strong systemic T-cell activation (Supplementary Figure S5). In anticipation of potential cytokine-related adverse effects, the patient received tocilizumab (IL-6 R blockade) and etanercept (TNF inhibitor) prophylactically. These were well tolerated, and no immune-mediated organ dysfunction, neurotoxicity, or autoimmune phenomena were observed.

The clinical deterioration observed on Day + 1 post-TIL-1 (KPS decline to 40) was attributed to peritumoral edema and mass effect rather than systemic toxicity. This was managed with urgent surgical decompression, with subsequent clinical improvement. No surgical complications occurred during or after any of the resection procedures.

No clinical or laboratory evidence of anaphylaxis, hypersensitivity reactions, or immediate-type immune responses was observed following either TIL infusion. Vital signs remained stable during and after infusion, and the patient did not develop rash, bronchospasm, hypotension, or signs of systemic allergic response. Furthermore, no signs of immune tolerance or blunted inflammatory response were observed with the second infusion. Instead, serum biomarkers, including IL-6 and soluble IL-2 receptor (sIL-2 R), showed marked increases after both TIL-1 and TIL-2, indicating preserved systemic immune activation. These findings suggest that repeated TIL administration did not induce immune desensitization or tolerogenic responses in this patient.

TIL phenotype and function

FACS analysis revealed that both TIL products comprised mostly of CD3⁺CD8⁺ T-cells, with almost no presence of NK-cells or Tregs (Figure 1B). 65% of the TILs, mostly CD8+ T-cells, were CD107a+ and presented high IFN-γ production (Figure 1C). Both TIL preparations specifically lysed the autologous tumor cell line (ATCL) in a dose-dependent manner (Figure 1D), but not the autologous EBV-transformed B-cell line. Highest TIL activity was observed when a greater number of T-cells were present in the control co-culture with the ATCL alone and dropped in a dose-dependent manner. Conversely, no TIL activity could be observed when the "cold ATCL" had been pre-incubated with the "hot ATCL" prior to the target inhibition assay, indicating a tumor-specific direct killing (Figure 1E)

Immuno-monitoring of circulating T-cells

After TIL infusion, peripheral blood T-cells exhibited activation-associated TCR downregulation (CD3^{-low}, Figure 2A), followed by an increase of CD8⁺ T-cells (Figure 2B). Detailed phenotypic analysis of CD4⁺ T-cells revealed increases in T-helper (Th)1*, Th17, and Th2 cells, while conventional Th1 levels remained stable (Figure 2C). There was a prominent expansion of stem cell-like memory T-cells (Tscm) and central memory T-cells, both associated with long-term persistence and effector recall capacity (Figure 2C-F). Moderate increases were observed in effector memory and precursor-like T-cells, whereas terminally differentiated CD8⁺ T-cells were reduced (Figure 2D-F), suggesting a shift toward a less differentiated and more durable T-cell phenotype.

Concurrently, we assessed T-cell exhaustion³⁵ and apoptosis³⁶ markers to evaluate the functional persistence of infused lymphocytes. PD-1, transiently upregulated upon T-cell activation, and CD95, a marker of both activation and apoptosis susceptibility, were used as surrogates of recent antigen encounter. PD-1⁺ and CD95⁺ T-cells increased in circulation over time in both CD4⁺ and CD8⁺ compartments, consistent with ongoing stimulation and activation-induced cell death (Figure 2G-I). LAG-3 expression remained unchanged, while CD57⁺ senescent cells increased slightly among CD8⁺ T-cells but decreased within CD4⁺ T-cells, suggesting limited terminal exhaustion. CD3^{-low} T-cells showed increased PD-1 and CD95 expression, consistent with recent antigen engagement, while CD3^{-low}CD57⁺ cells decreased and LAG-3 remained undetectable. Collectively, these findings indicate a dynamic, activated T-cell compartment with preserved memory and limited exhaustion, supporting functional persistence of the infused TILs.

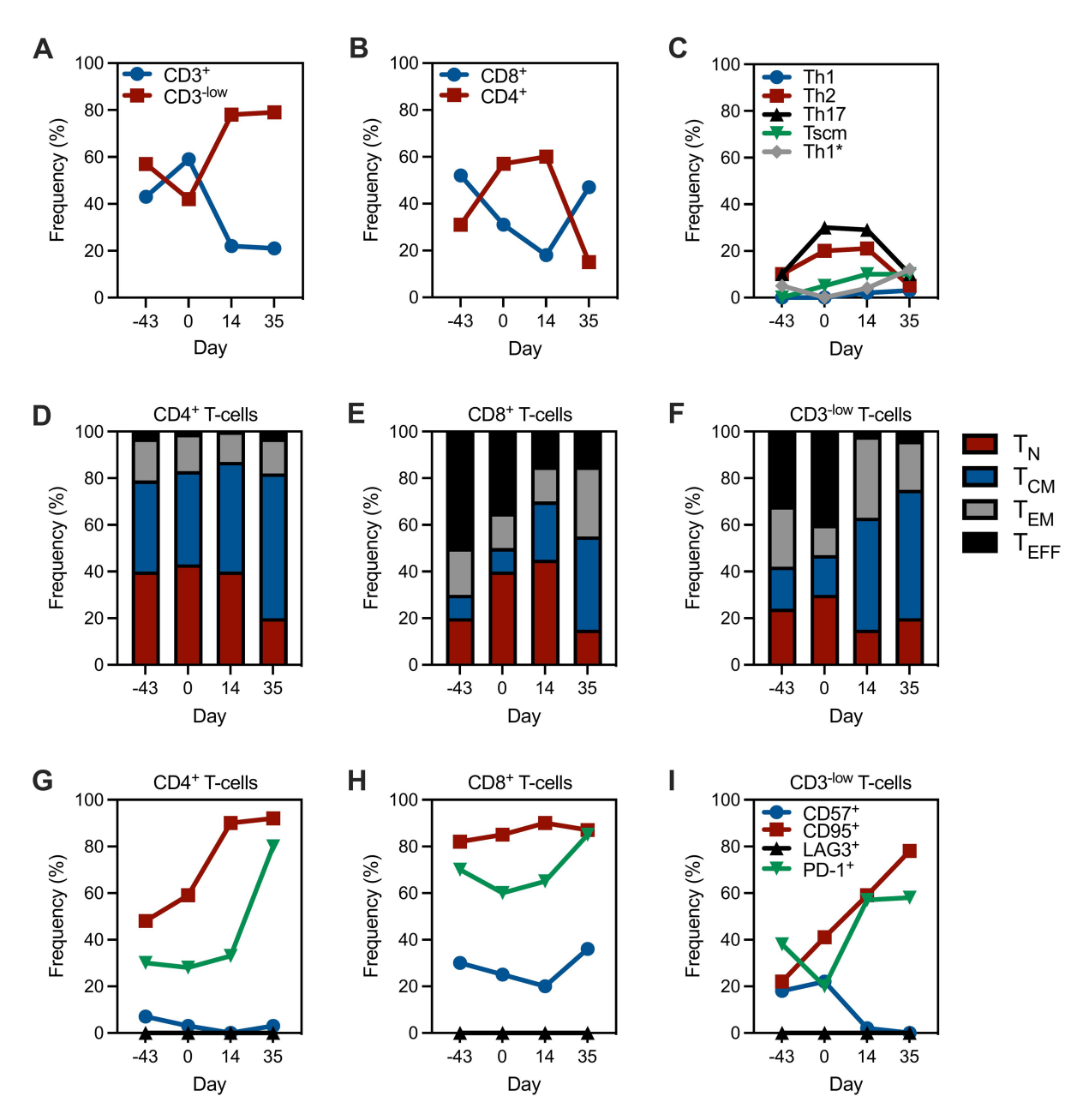


Figure 2. Peripheral blood T-cell immunophenotype analysis over the course of TIL therapy. Flow cytometric analysis of (A) total CD3⁺/CD3^{-low} and (B) CD4⁺/CD8⁺ T-cells before and after TIL treatment. CD3^{-low} T-cells represent T-cells with downregulated TCR complex due to activation. (C) Changes on CD4⁺ T-helper (Th) subtypes frequency post-treatment. Th subtypes is based on CXCR3/CCR4/CCR6 surface expression: Th1 (CXCR3⁺CCR6⁻CCR4⁻), Th2 (CCR4⁺CXCR3⁻CCR6⁻), Th17 (CCR4⁺CXCR3⁻) and nonconventional Th1* (CXCR3⁺CCR6⁺CCR4⁻). Changes on naïve (CCR7⁺CD45RA⁺, T_N), central memory (CCR7⁺CD45RA⁻, T_{CM}), effector memory (CCR7⁻CD45RA⁻, T_{EM}) and fully differentiated effector (CCR7⁻CD45RA⁺, T_{EFF}) subtypes before and after TIL therapy in (D) CD4⁺, (E) CD8⁺ and (F) CD3^{-low} T-cells. Expressions of CD57, CD95, LAG3 and PD-1 before and after TIL therapy by (G) CD4⁺, (H) CD8⁺ and (I) CD3^{-low} T-cells.

Multi-omics

Surgical tumor samples (Figure 1A) underwent whole-exome sequencing, revealing a high baseline mutation burden (> 10 mutations/Mb, Figure 3A) that increased during TIL therapy, along with the number of mutated genes (Figure 3B) and total mutations (Figure 3C). Of note, mutations on EGFR, TP53 and BRCA1/2 were found in all samples, highlighting their potential role in glioblastoma progression and response to TIL therapy.

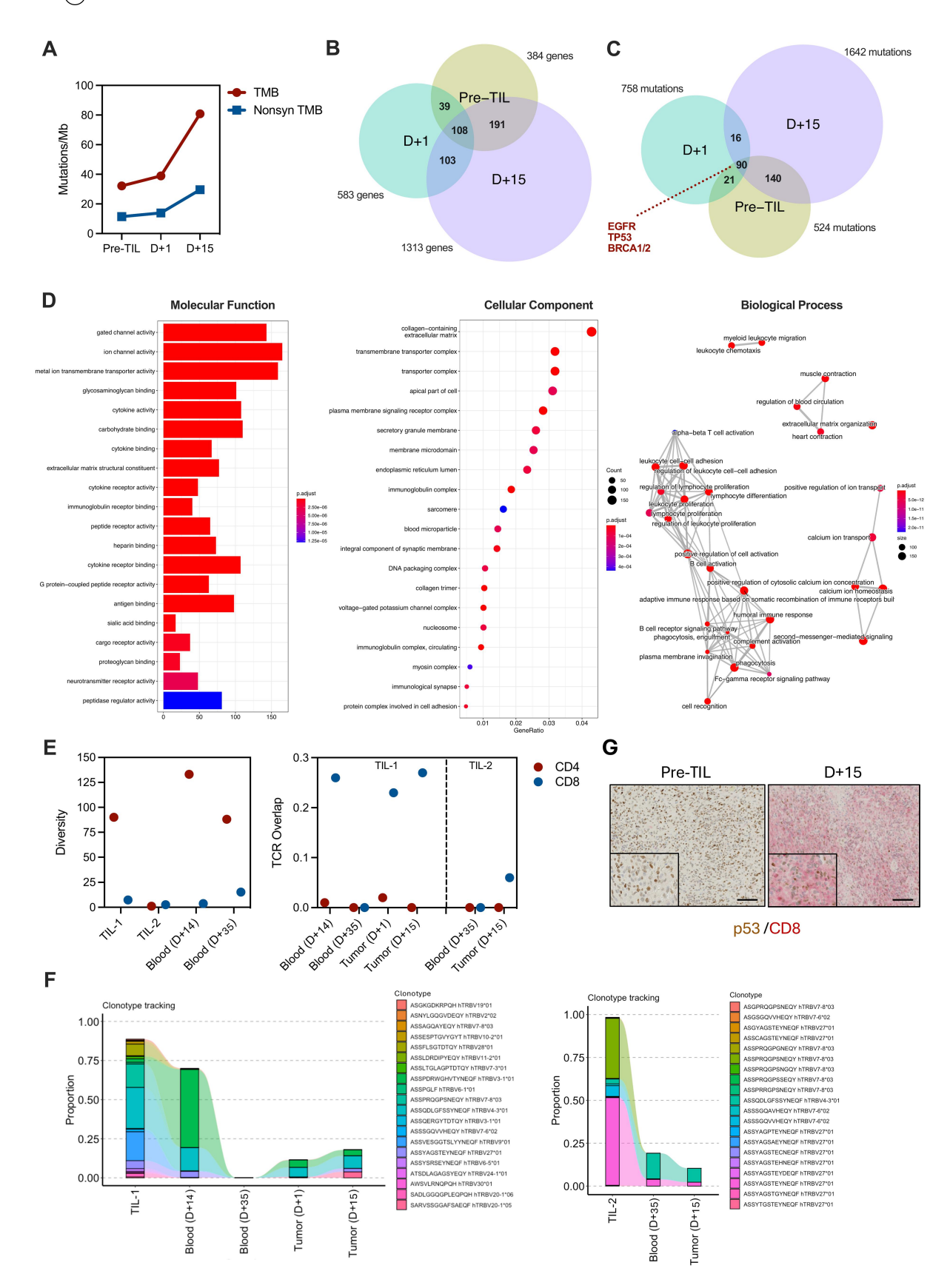


Figure 3. WES, transcriptomics and TCR NGS. (A) Tumor mutation burden (TMB) analysis before and after therapy expressed as number of mutations per megabase (mb) of the genome. Total TMB is depicted in red, while non-synonymous mutations are in blue. The Venn-diagrams depict the number of mutated genes (B) and the number of individual mutations (C) detected in each sample and across samples. Highlighted are key driver mutations found in all analyzed samples (EGFR,

A high TMB in gliomas has not been reported to correlate with better survival outcomes in response to immunotherapy, ¹¹ therefore we aimed at investigating the pharmacodynamics and pharmacokinetics of the infused TIL product. Transcriptomic analysis of tumor tissue collected post-TIL therapy demonstrated an enrichment of genes related to immunological synapse and T-cell effector function (Figure 3D), suggestive of T-cell-mediated tumor clearance.

We therefore used TCR NGS to check the infiltration of TIL-derived clonotypes into the tumor tissue.³⁷ TIL-derived CD4⁺ T-cells, despite showing higher TCR diversity than CD8⁺ counterparts, presented low persistence and tumor infiltration (Figure 3E). TIL-derived CD8⁺ T-cells efficiently infiltrated the tumor tissue (Figure 3E,F) and is closely associated with the clearance of tumor cells (Figure 3G). This is further confirmed by the presence of overrepresented TIL-derived clonotypes in the tumor tissue (Figure 4A), resulting in higher presence of hyperexpanded clones in the tumor tissue (Figure 4B) as consequence of TIL-derived CD8⁺ T-cell expansion in the tumor tissue (Figure 4C). We next investigated whether IL-2 treatment following TIL infusion drives significant *in situ* clonotype expansion. When tracking the most abundant clonotypes from the pre-TIL tumor specimen, we found that the majority were either undetectable in post-TIL tumor samples or had contracted significantly (Figure 4D). Clonotypes identified in post-TIL tumor samples were classified as expanded or contracted based on significant changes in their relative proportions compared to the infused TIL product or to the pre-treatment tumor sample. Notably, 65.8% of TIL-derived CD8⁺ clonotypes exhibited expansion, whereas tumor-derived clonotypes primarily contracted over the course of therapy (Figure 4E,F). These findings indicate that TIL-derived CD8+ T-cells successfully infiltrated the tumor, expanded, and contributed to tumor clearance

Discussion

This case report demonstrates the feasibility, safety and potential efficacy of intravenous IL-2/IL-15/IL-21-expanded TILs administration in a patient with recurrent, treatment-refractory GBM. Despite the traditionally poor responsiveness of GBM to immunotherapy due to its highly immunosuppressive microenvironment, low T-cell infiltration, and dysfunctional antigen presentation, ¹¹ the patient experienced tumor regression and clonotypic T-cell expansion following TIL therapy.

The preparatory regimen used in this study with a single-dose cyclophosphamide differs substantially from the standard lymphodepletion protocols employed in most TIL studies, which typically involve two doses of cyclophosphamide followed by five days of fludarabine prior to TIL infusion. ^{1–4,17,38,39} High-dose conditioning induces significant lymphopenia, usually prompting the production of endogenous IL-7 and IL-15, homeostatic cytokines that can further stimulate transferred TIL in the lymphopenic host. ⁴⁰ The reduced-intensity conditioning regimen induced mild lymphopenia and moderate neutropenia but did not result in complete lymphodepletion. Despite this, the patient experienced clinical improvement, and TCR sequencing revealed a high level of circulating TIL-derived clonotypes two weeks post-infusion, indicating that the conditioning regimen did not impair TIL expansion or persistence. These findings support previous observations that reduced-intensity lymphodepletion may be sufficient to facilitate TIL engraftment in some patients, while minimizing the toxicity associated with high-dose conditioning regimens. ³¹

Despite the relative low TIL numbers used for infusion (0.7 and 2.1×10^9 cells) and a short two-week interval between the infusions, a single post-transfer dose of IL-2 provided sufficient support. Multi-omics data showed that the intravenously administered TILs successfully crossed the BBB, with increasing

TP53 and BRCA1/2). (D) Gene ontogeny analysis comparing differentially expressed genes after TIL treatment (day \pm 15) as compared to baseline. Note the enrichment of processes associated with T-cell activation and effector function. The Y-axis represents gene functions, and the X-axis represents gene counts and ratios. Each bar or circles/nodes represents a different enrichment function, and the significance threshold was set to adjusted p < 0.05. (E) *Left panel*, TCR diversity as calculated by the inverse Simpson's index of sorted CD4⁺ and CD8⁺ T-cells from TIL products and blood samples after TIL therapy. *right panel*, morisita-horn overlap index between CD4/CD8 T-cells isolated from the TIL products and blood samples or tumor-infiltrating T-cells. (F) Clonotype tracking of the top 20 most frequent CDR3 amino acid sequences from TIL-1 (*left panel*) and TIL-2 (*right panel*) CD8⁺ T-cells in the blood and tumor tissue after TIL therapy. Clonotypes are not colour coded between panels. (G) Dual immunohistochemistry of p53 (brown) and CD8 (red) in a tumor sample collected before TIL treatment and at day + 15 post infusion (scale bar, 100 µm).

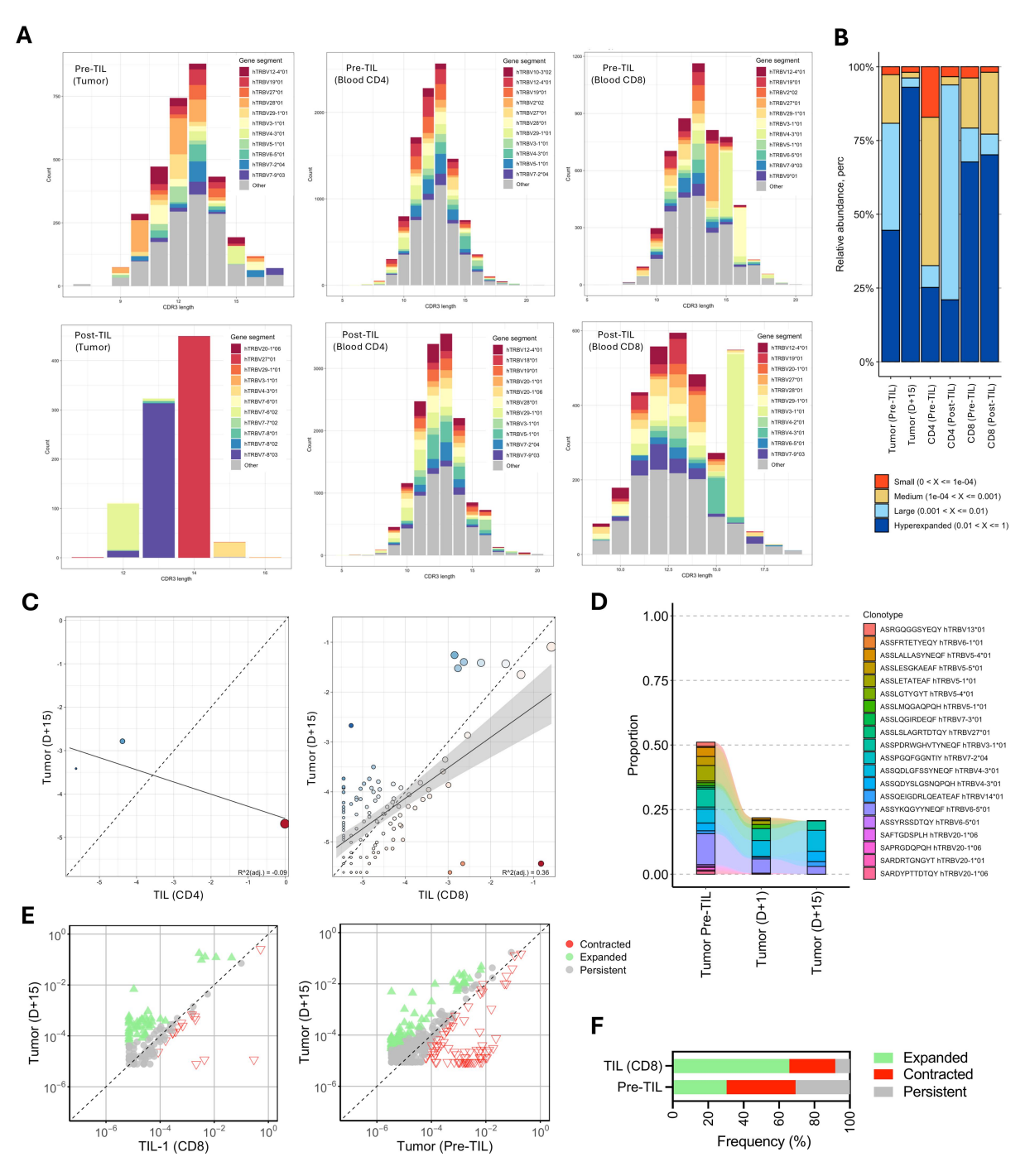


Figure 4. CD8⁺ TIL-derived clonotypes infiltrate the tumor tissue after TIL therapy. (A) CDR3 spectratype of tumor and TIL/blood samples (sorted CD4⁺ and CD8⁺ fractions) before and after TIL treatment (day +15). Bars represent counts of unique CDR3 sequences with different amino acid lengths. Most frequent variable gene segments are highlighted within each sample and is not color coded across different samples. (B) Proportion of homeostatic space occupied by clonotypes classified as hyperexpanded (1–100%), large (0.1–1%), medium (0.01–0.1%) and small (0–0.01%) from tumor and TIL/blood samples (sorted CD4⁺ and CD8⁺ fractions) before and after TIL treatment (day +15). (C) TCR repertoire overlap scatterplot depicting the CDR3 sequences overlapping between sorted CD4 or CD8 T-cells from TIL-1 product and infiltrating T-cells within the tumor tissue at day + 15. Point size is scaled to the clonotype abundance and the axes represent \log_{10} clonotype frequencies in each sample. R² represents squared Pearson's correlation coefficient of the linear regression of overlapping clonotypes. (D) Clonotype tracking of the top 20 most frequent clonotypes in the tumor before TIL treatment, showing their proportion in the tumor samples collected after TIL infusions. (E) Clonotype abundance analysis of public clonotypes present in the tumor after treatment. CDR3 sequences were classified as 'contracted' or 'expanded' based on a Fisher's exact test (p < 0.01) comparing the tumor sample to either the TIL-1 product (left panel) or the pre-treatment tumor specimen (right panel). (F) Proportion of clonotypes classified as expanded, contracted or persistent.

proportions of TIL-derived CD8⁺ clonotypes detected in the tumor tissue over time, indicating effective homing and intratumoral expansion without the need for repeated IL-2 dosing. 17 These findings suggest that limited IL-2 support may be sufficient to promote TIL persistence and antitumor activity, as demonstrated by the robust expansion of TIL-derived clonotypes in both peripheral blood and tumor tissue, reflecting functional competence and long-term engraftment. There is currently no consensus on the optimal IL-2 dosing regimen, as studies have shown no clear difference in IL-2 exposure between responders and non-responders.⁴¹

Similar positive outcomes were observed in a prostate cancer patient treated with IL-2/IL-15/IL-21-expanded TILs through repeated low-dose infusions, resulting in long-term complete remission.²² This suggests that multiple TIL administrations may enhance the pharmacokinetic and pharmacodynamic profile of the therapy, a strategy that has also been associated with improved responses in CAR T-cell treatments. 42 A potential concern with repeated adoptive T-cell therapies is the risk of immune tolerance, desensitization, or anaphylaxis upon reexposure. However, no clinical or laboratory signs of such phenomena were detected. The second TIL infusion was well tolerated and provoked a similarly robust systemic immune response as the first, as evidenced by IL-6 and sIL-2 R surges, persistent TCR engagement, and expansion of memory T-cell subsets. This supports the feasibility of iterative TIL dosing without inducing immune exhaustion or tolerance, and may reflect the functional advantages conferred by IL-2/IL-15/IL-21-expanded TILs. 43,44

The patient's clinical deterioration following the first TIL infusion was attributed to peritumoral edema and mass effect, rather than systemic toxicity, and was successfully managed with urgent decompressive surgery. Following stabilization, a second infusion was administered, resulting in further radiologic tumor reduction and tumor necrosis. Similar to previously reported cases of locally administered TILs, posttreatment imaging revealed hyperemia and swelling in all responding patients, consistent with a transient "flare" response likely reflecting cerebral edema and increased vascular perfusion. 19 IL-6-bloking therapy was administered 24 hours after infusion to counteract the compartmentalized inflammation, 12 leading to a rapid decline in IL-6 levels and mitigating further immune-related toxicity. Transcriptomic data revealed T-cell activation signatures, and TCR sequencing confirmed clonal expansion of infused TILs within the tumor, supporting their direct involvement in mediating tumor regression. While concurrent interventions (e.g., conditioning chemotherapy, IL-2 administration, anti-cytokine therapy, surgery) may have contributed to clinical recovery, the temporal sequence and molecular tracking of TIL clonotypes suggest that the TIL product mediated the observed tumor regression.

While PD-1 expression on TILs can reflect both exhaustion and chronic activation, studies in GBM have shown that PD-1 expression on peripheral blood T cells more commonly indicates recent antigen experience and sustained activation rather than terminal dysfunction, retaining cytotoxic potential.³⁵ Similarly, elevated CD95 expression on circulating lymphocytes has been associated with improved survival in GBM.³⁶ In our study, both PD-1 and CD95 levels increased following TIL infusion, particularly within the CD3^{low} population, consistent with ongoing antigen engagement. The low expression of LAG-3 and absence of CD57 accumulation suggest limited terminal exhaustion or senescence. These findings support the interpretation of PD-1 as a dynamic marker of activation in the context of adoptive T-cell therapy, with implications for its use as a pharmacodynamic biomarker and in guiding checkpoint blockade strategies.

In conclusion, adoptive transfer of IL-2/IL-15/IL-21-expanded TILs represents a promising and potentially transformative approach for immunologically "cold" tumors such as GBM. This case demonstrates that effective tumor control can be achieved with substantially lower TIL doses than previously reported, 1-4,17,38,39 supporting the feasibility of faster TIL manufacturing without compromising antitumor activity. The results also underscore the importance of personalized immunotherapy strategies, multidisciplinary coordination, and longitudinal immune monitoring to assess treatment response and safety. Multiple, temporally spaced TIL infusions may enhance therapeutic outcomes by prolonging TIL-tumor interactions while reducing toxicity associated with single high-dose regimens. Moving forward, prospective trials incorporating systemic TIL therapy, non-myeloablative conditioning, and real-time immunogenomic tracking will be essential to validate these findings and optimize treatment protocols.

Acknowledgments

The authors would like to thank Claudia Wahle for excellent tumor- and T-cell culturing, and the Champalimaud Foundation for the support with the multi-omics and flow cytometry data.

Author contributions

CRediT: Lucas C. M. Arruda: Conceptualization, Data curation, Formal analysis, Funding acquisition, Investigation, Methodology, Software, Writing – original draft, Writing – review & editing; Julia Karbach: Conceptualization, Data curation, Formal analysis, Investigation, Methodology, Project administration, Writing – review & editing; Dragan Kiselicki: Data curation, Methodology, Supervision, Writing – review & editing; Hans-Michael Altmannsberger: Data curation, Investigation, Methodology, Writing – review & editing; Evgueni Sinelnikov: Formal analysis, Methodology, Validation, Writing – review & editing; Dirk Gustavus: Data curation, Formal analysis, Methodology, Validation, Writing – review & editing; Hans Hoffmeister: Conceptualization, Data curation, Project administration, Resources, Supervision, Writing – original draft, Writing – review & editing; Akin Atmaca: Formal analysis, Methodology, Writing – review & editing; Elke Jäger: Conceptualization, Data curation, Formal analysis, Funding acquisition, Investigation, Methodology, Project administration, Resources, Supervision, Writing – original draft, Writing – review & editing.

Disclosure statement

L.C.M.A is an employee of CuraCell Holding AB. J.K. and E.J. are consultants of CuraCell Holding AB. E. S., D. G. and H. H. are employees of Zellwerk GmbH. The authors declare that they have no other competing interests.

Funding

This work was funded by CuraCell Holding AB through internal research and development resources.

ORCID

Lucas C. M. Arruda (b) http://orcid.org/0000-0002-8573-9618

Data availability statement

WES, TCR and RNA and sequencing data generated in this study are publicly available in Gene Expression Omnibus at GSE285283, GSE285282 and GSE285281 respectively. All other raw data generated in this study are available upon request from the corresponding author.

References

- 1. Martín-Lluesma S, Svane IM, Dafni U, Vervita K, Karlis D, Dimopoulou G, Tsourti Z, Rohaan MW, Haanen JBAG, Coukos G. Efficacy of TIL therapy in advanced cutaneous melanoma in the current immuno-oncology era: updated systematic review and meta-analysis. Ann Oncol. 2024;35(10):860–872. doi: 10.1016/j.annonc.2024.07.723.
- 2. Tran E, Robbins PF, Lu Y-C, Prickett TD, Gartner JJ, Jia L, Pasetto A, Zheng Z, Ray S, Groh EM, et al. T-cell transfer therapy targeting mutant KRAS in cancer. N Engl J Med. 2016;375(23):2255–2262. doi: 10.1056/NEJMoa1609279.
- 3. Creelan BC, Wang C, Teer JK, Toloza EM, Yao J, Kim S, Landin AM, Mullinax JE, Saller JJ, Saltos AN, et al. Tumor-infiltrating lymphocyte treatment for anti-PD-1-resistant metastatic lung cancer: a phase 1 trial. Nat Med. 2021;27(8):1410–1418. doi: 10.1038/s41591-021-01462-y.
- 4. Rohaan MW, Borch TH, van den Berg JH, Met Ö, Kessels R, Geukes Foppen MH, Stoltenborg Granhøj J, Nuijen B, Nijenhuis C, Jedema I, et al. Tumor-infiltrating lymphocyte therapy or ipilimumab in advanced melanoma. NEJM evid. 2022;387(23):2113–2125. doi: 10.1056/NEJMoa2210233.
- 5. Weller M, van den Bent M, Preusser M, Le Rhun E, Tonn JC, Minniti G, Bendszus M, Balana C, Chinot O, Dirven L, et al. EANO guidelines on the diagnosis and treatment of diffuse gliomas of adulthood. Nat Rev Clin Oncol. 2021;18(3):170–186. doi: 10.1038/s41571-020-00447-z.



- 6. Stupp R, Mason WP, van den Bent MJ, Weller M, Fisher B, Taphoorn MJB, Belanger K, Brandes AA, Marosi C, Bogdahn U, et al. Radiotherapy plus concomitant and adjuvant temozolomide for glioblastoma. NEJM Evid. 2005;352(10):987-996. doi: 10.1056/NEJMoa043330 .
- 7. Liu Y, Zhou F, Ali H, Lathia JD, Chen P. Immunotherapy for glioblastoma: current state, challenges, and future perspectives. Cell Mol Immunol. 2024;21(12):1354-1375. doi: 10.1038/s41423-024-01226-x.
- 8. Omuro A, Brandes AA, Carpentier AF, Idbaih A, Reardon DA, Cloughesy T, Sumrall A, Baehring J, van den Bent M, Bähr O, et al. Radiotherapy combined with nivolumab or temozolomide for newly diagnosed glioblastoma with unmethylated MGMT promoter: an international randomized phase III trial. Neuro Oncol. 2023;25 (1):123-134. doi: 10.1093/neuonc/noac099.
- 9. Xiong Z, Raphael I, Olin M, Okada H, Li X, Kohanbash G. Glioblastoma vaccines: past, present, and opportunities. EBioMedicine. 2024;100:104963. doi: 10.1016/j.ebiom.2023.104963.
- 10. Narita Y, Arakawa Y, Yamasaki F, Nishikawa R, Aoki T, Kanamori M, Nagane M, Kumabe T, Hirose Y, Ichikawa T, et al. A randomized, double-blind, phase III trial of personalized peptide vaccination for recurrent glioblastoma. Neuro Oncol. 2019;21(3):348-359. doi: 10.1093/neuonc/nov200.
- 11. Merchant M, Ranjan A, Pang Y, Yu G, Kim O, Khan J, Wu J. Tumor mutational burden and immunotherapy in gliomas. Trends Cancer. 2021;7(12):1054-1058. doi: 10.1016/j.trecan.2021.08.005.
- 12. O'Rourke DM, Nasrallah MP, Desai A, Melenhorst JJ, Mansfield K, Morrissette JJD, Martinez-Lage M, Brem S, Maloney E, Shen A, et al. A single dose of peripherally infused EGFRvIII-directed CAR T cells mediates antigen loss and induces adaptive resistance in patients with recurrent glioblastoma. Sci Transl Med. 2017;9(399). doi: 10. 1126/scitranslmed.aaa0984.
- 13. Bagley SJ, Logun M, Fraietta JA, Wang X, Desai AS, Bagley LJ, Nabavizadeh A, Jarocha D, Martins R, Maloney E, et al. Intrathecal bivalent CAR T cells targeting EGFR and IL13Rα2 in recurrent glioblastoma: phase 1 trial interim results. Nat Med. 2024;30(5):1320-1329. doi: 10.1038/s41591-024-02893-z.
- 14. Choi BD, Gerstner ER, Frigault MJ, Leick MB, Mount CW, Balaj L, Nikiforow S, Carter BS, Curry WT, Gallagher K, et al. Intraventricular CARv3-TEAM-E T cells in recurrent glioblastoma. NEJM Evid. 2024;390 (14):1290-1298. doi: 10.1056/NEJMoa2314390.
- 15. Brown CE, Hibbard JC, Alizadeh D, Blanchard MS, Natri HM, Wang D, Ostberg JR, Aguilar B, Wagner JR, Paul JA, et al. Locoregional delivery of IL-13Rα2-targeting CAR-T cells in recurrent high-grade glioma: a phase 1 trial. Nat Med. 2024;30(4):1001-1012. doi: 10.1038/s41591-024-02875-1.
- 16. Vitanza NA, Ronsley R, Choe M, Seidel K, Huang W, Rawlings-Rhea SD, Beam M, Steinmetzer L, Wilson AL, Brown C, et al. Intracerebroventricular B7-H3-targeting CAR T cells for diffuse intrinsic pontine glioma: a phase 1 trial. Nat Med. 2025;31(3):861-868. doi: 10.1038/s41591-024-03451-3.
- 17. Albarrán Fernández V, Ballestín Martínez P, Stoltenborg Granhøj J, Borch TH, Donia M, Marie Svane I. Biomarkers for response to TIL therapy: a comprehensive review. J Immunother Cancer. 2024;12(3):e008640. doi: 10.1136/jitc-2023-008640.
- 18. Kristensen NP, Heeke C, Tvingsholm SA, Borch A, Draghi A, Crowther MD, Carri I, Munk KK, Holm JS, Bjerregaard A-M, et al. Neoantigen-reactive CD8+ T cells affect clinical outcome of adoptive cell therapy with tumor-infiltrating lymphocytes in melanoma. J Clin Invest. 2022;132(2). doi: 10.1172/JCI150535.
- 19. Quattrocchi KB, Miller CH, Cush S, Bernard SA, Dull ST, Smith M, Gudeman S, Varia MA. Pilot study of local autologous tumor infiltrating lymphocytes for the treatment of recurrent malignant gliomas. J Neurooncol. 1999;45(2):141-157. doi: 10.1023/A:1006293606710.
- 20. Albrecht HC, Gustavus D, Schwanemann J, Dammermann W, Lippek F, Weylandt K-H, Hoffmeister H, Gretschel S. Generation of colon cancer-derived tumor-infiltrating T cells (TILs) for adoptive cell therapy. Cytotherapy. 2023;25(5):537–547. doi: 10.1016/j.jcyt.2023.01.009.
- 21. Becattini S, Latorre D, Mele F, Foglierini M, De Gregorio C, Cassotta A, Fernandez B, Kelderman S, Schumacher TN, Corti D, et al. Functional heterogeneity of human memory CD4 + T cell clones primed by pathogens or vaccines. Science (1979). 2015;347(6220):400-406. doi: 10.1126/science.1260668.
- 22. Karbach J, Kiselicki D, Brand K, Wahle C, Sinelnikov E, Gustavus D, Hoffmeister H, Prisack H-B, Atmaca A, Jäger E. Tumor-infiltrating lymphocytes mediate complete and durable remission in a patient with NY-ESO-1 expressing prostate cancer. J Immunother Cancer. 2023;11(1):e005847. doi: 10.1136/jitc-2022-005847.
- 23. Cock PJA, Fields CJ, Goto N, Heuer ML, Rice PM. The Sanger FASTQ file format for sequences with quality scores, and the Solexa/Illumina FASTQ variants. Nucleic Acids Res. 2010;38(6):1767-1771. doi: 10.1093/nar/ gkp1137.
- 24. Jiang H, Lei R, Ding S-W, Zhu S. Skewer: a fast and accurate adapter trimmer for next-generation sequencing paired-end reads. BMC BioInf. 2014;15(1):182. doi: 10.1186/1471-2105-15-182.
- 25. Danecek P, Auton A, Abecasis G, Albers CA, Banks E, DePristo MA, Handsaker RE, Lunter G, Marth GT, Sherry ST, et al. The variant call format and VCFtools. Bioinformatics. 2011;27(15):2156-2158. doi: 10.1093/ bioinformatics/btr330.
- 26. Dobin A, Davis CA, Schlesinger F, Drenkow J, Zaleski C, Jha S, Batut P, Chaisson M, Gingeras TR. Star: ultrafast universal RNA-seq aligner. Bioinformatics. 2013;29(1):15-21. doi: 10.1093/bioinformatics/bts635.
- 27. Love MI, Huber W, Anders S. Moderated estimation of fold change and dispersion for RNA-seq data with DESeq2. Genome Biol. 2014;15(12):550. doi: 10.1186/s13059-014-0550-8.



- 28. Ashburner M, Ball CA, Blake JA, Botstein D, Butler H, Cherry JM, Davis AP, Dolinski K, Dwight SS, Eppig JT, et al. Gene Ontology: tool for the unification of biology. Nat Genet. 2000;25(1):25-29. doi: 10.1038/75556.
- 29. Wu T, Hu E, Xu S, Chen M, Guo P, Dai Z, Feng T, Zhou L, Tang W, Zhan L, et al. Clusterprofiler 4.0: a universal enrichment tool for interpreting omics data. Innovation. 2021;2(3):100141. doi: 10.1016/j.xinn.2021.100141.
- 30. Wang C, Sanders CM, Yang Q, Schroeder HW, Wang E, Babrzadeh F, Gharizadeh B, Myers RM, Hudson JR, Davis RW, et al. High throughput sequencing reveals a complex pattern of dynamic interrelationships among human T cell subsets. Proc Natl Acad Sci, India, Sect B Biol Sci. 2010;107(4):1518-1523. doi: 10.1073/pnas. 0913939107.
- 31. Nissani A, Lev-Ari S, Meirson T, Jacoby E, Asher N, Ben-Betzalel G, Itzhaki O, Shapira-Frommer R, Schachter J, Markel G, et al. Comparison of non-myeloablative lymphodepleting preconditioning regimens in patients undergoing adoptive T cell therapy. J Immunother Cancer. 2021;9(5):e001743. doi: 10.1136/jitc-2020-001743.
- 32. Turcotte S, Donia M, Gastman B, Besser M, Brown R, Coukos G, Creelan B, Mullinax J, Sondak VK, Yang JC, et al. Art of TIL immunotherapy: SITC's perspective on demystifying a complex treatment. J Immunother Cancer. 2025;13(1):e010207. doi: 10.1136/jitc-2024-010207.
- 33. Le RQ, Li L, Yuan W, Shord SS, Nie L, Habtemariam BA, Przepiorka D, Farrell AT, Pazdur R. Fda approval summary: tocilizumab for treatment of chimeric antigen receptor T cell-induced severe or life-threatening cytokine release syndrome. Oncologist. 2018;23(8):943-947. doi: 10.1634/theoncologist.2018-0028.
- 34. Okada H, Weller M, Huang R, Finocchiaro G, Gilbert MR, Wick W, Ellingson BM, Hashimoto N, Pollack IF, Brandes AA, et al. Immunotherapy response assessment in neuro-oncology: a report of the RANO working group. Lancet Oncol. 2015;16(15):e534-e542. doi: 10.1016/S1470-2045(15)00088-1.
- 35. Davidson TB, Lee A, Hsu M, Sedighim S, Orpilla J, Treger J, Mastall M, Roesch S, Rapp C, Galvez M, et al. Expression of PD-1 by T cells in malignant glioma patients reflects exhaustion and activation. Clin Cancer Res. 2019;25(6):1913-1922. doi: 10.1158/1078-0432.CCR-18-1176.
- 36. Mostafa H, Pala A, Högel J, Hlavac M, Dietrich E, Westhoff MA, Nonnenmacher L, Burster T, Georgieff M, Wirtz CR, et al. Immune phenotypes predict survival in patients with glioblastoma multiforme. J Hematol Oncol. 2016;9(1):77. doi: 10.1186/s13045-016-0272-3.
- 37. Hsu MS, Sedighim S, Wang T, Antonios JP, Everson RG, Tucker AM, Du L, Emerson R, Yusko E, Sanders C, et al. Tcr sequencing can identify and track glioma-infiltrating T cells after dc vaccination. Cancer Immunol Res. 2016;4(5):412-418. doi: 10.1158/2326-6066.CIR-15-0240.
- 38. Rosenberg SA, Yang JC, Sherry RM, Kammula US, Hughes MS, Phan GQ, Citrin DE, Restifo NP, Robbins PF, Wunderlich JR, et al. Durable complete responses in heavily pretreated patients with metastatic melanoma using T-cell transfer immunotherapy. Clin Cancer Res. 2011;17(13):4550-4557. doi: 10.1158/1078-0432.CCR-11-0116.
- 39. Rosenberg SA, Restifo NP. Adoptive cell transfer as personalized immunotherapy for human cancer. Science (1979). 2015;348(6230):62-68. doi: 10.1126/science.aaa4967.
- 40. Dudley ME, Yang JC, Sherry R, Hughes MS, Royal R, Kammula U, Robbins PF, Huang J, Citrin DE, Leitman SF, et al. Adoptive cell therapy for patients with metastatic melanoma: evaluation of intensive myeloablative chemoradiation preparative regimens. J Clin Oncol. 2008;26(32):5233-5239. doi: 10.1200/JCO.2008.16.5449.
- 41. Seitter SJ, Sherry RM, Yang JC, Robbins PF, Shindorf ML, Copeland AR, McGowan CT, Epstein M, Shelton TE, Langhan MM. Impact of prior treatment on the efficacy of adoptive transfer of tumor-infiltrating lymphocytes in patients with metastatic melanoma. Clin Cancer Res. 2021;27 (19):5289-5298. doi: 10.1158/1078-0432.CCR-21-1171.
- 42. Kirouac DC, Zmurchok C, Morris D. Making drugs from T cells: the quantitative pharmacology of engineered T cell therapeutics. NPJ Syst Biol Appl. 2024;10(1):31. doi: 10.1038/s41540-024-00355-3.
- 43. Pouw N, Treffers-Westerlaken E, Kraan J, Wittink F, ten Hagen T, Verweij J, Debets R. Combination of IL-21 and IL-15 enhances tumour-specific cytotoxicity and cytokine production of TCR-transduced primary T cells. Cancer Immunol Immun. 2010;59(6):921-931. doi: 10.1007/s00262-010-0818-0.
- 44. Moroz A, Eppolito C, Li Q, Tao J, Clegg CH, Shrikant PA. Il-21 enhances and sustains CD8+ T cell responses to achieve durable tumor immunity: comparative evaluation of IL-2, IL-15, and IL-21. J Immunol. 2004;173 (2):900-909. doi: 10.4049/jimmunol.173.2.900.